Fast Cell Discovery in mm-wave 5G Networks with Context Information

Ilario Filippini, *Senior Member, IEEE,* Vincenzo Sciancalepore, *Member, IEEE,* Francesco Devoti, and Antonio Capone, *Senior Member, IEEE*

Abstract—The exploitation of mm-wave bands is one of the key-enabler for 5G mobile radio networks. However, the introduction of mm-wave technologies in cellular networks is not straightforward due to harsh propagation conditions that limit the mm-wave access availability. Mm-wave technologies require high-gain antenna systems to compensate for high path loss and limited power. As a consequence, directional transmissions must be used for cell discovery and synchronization processes: this can lead to a non-negligible access delay caused by the exploration of the cell area with multiple transmissions along different directions.
The integration of mm-wave technologies and conventional wireless access networks with the objective of speeding up the cell search process requires new 5G network architectural solutions. Such architectures introduce a functional split between C-plane and U-plane, thereby guaranteeing the availability of a reliable signaling channel through conventional wireless technologies that provides the opportunity to collect useful context information from the network edge.
In this article, we leverage the context information related to user positions to improve the directional cell discovery process. We investigate fundamental trade-offs of this process and the effects of the context information accuracy on the overall system performance. We also cope with obstacle obstructions in the cell area and propose an approach based on a geo-located context database where information gathered over time is stored to guide future searches. Analytic models and numerical results are provided to validate proposed strategies.

Index Terms—5G networks, mm-wave radio access, RAN, directional cell discovery, context information, obstacle shadowing, reflected paths.

1 Introduction

In this phase of the process that will lead to the definition of the 5th generation (5G) of wireless access networks, the mobile industry sector is facing a traffic demand revolution that is strongly impacting on the wireless network performance. Guaranteeing high peak rates and low latency requirements is no longer an option of few dedicated customers: advanced solutions must be developed to handle the enormous amount of user applications' requests, which are pushing operator networks to face wireless resource scarcity. In this context, the compelling availability of new big spectrum shares is drawing the attention of academic and industrial partners to explore frequencies above the conventional 5GHz. To this extent, a promising opportunity is represented by millimeter wave (mm-wave) communications, which give a two-fold advantage: i) additional unlicensed spectrum bands can be smartly turned to good account, ii) extremely wide bandwidths (up to 1GHz), enabling ultra-high data rates for greedy users [1].

Having been used for many years as a reference technology in point-to-point links, standardization groups are now approaching mm-wave exploitation from a different angle: the Radio Access Network (RAN) design. This opens up new challenges as mm-wave RAN technology might suffer from severe propagation losses combined with an adverse propagation environment. On the one hand, the weak ability to diffract around obstacles makes mm-wave communications vulnerable to blockage problems, as witnessed by the hard characterization of mm-wave channel models [2]. On the other hand, the short wavelength allows the use of antenna arrays with a relatively large number of elements accommodated in a small space, both on the base station (BS) and on the user's mobile terminal (MT) [1]. Therefore, the research trend in mm-wave transmission technologies is currently moving towards the use of advanced beamforming techniques to concentrate the overall radiated power on very small angles, so as to augment the transmission range (i.e., the cell coverage) and to easily track terminals upon they move within the coverage area. These techniques bring mm-wave small cells to cover up to a few hundreds of meters [3], [4].

Nonetheless, the integration of mm-wave small cells in the current legacy RAN architectures exhibits its major limitations. Even resorting to the most advanced beamforming techniques, a full mm-wave small-cell deployment presents critical service disruptions and signal losses due to the high attenuation and the presence of obstacles (including human bodies), which can seriously hamper the signal propagation. To overcome this issue, we rely on a cellular architecture based on heterogeneous layers that blends together the emerging SDN paradigm and the functional split between

- *Ilario Filippini, Francesco Devoti and Antonio Capone are with Politecnico di Milano, Dipartimento di Elettronica, Informazione e Bioingegneria, Piazza L. da Vinci, 32, 20133 Milan, Italy. E-mail: {name.surname}@polimi.it.*
- *Vincenzo Sciancalepore is with NEC Europe Ltd., Heidelberg, Germany. E-mail: vincenzo.sciancalepore@neclab.eu.*

1. Terms *user* and *mobile terminal* are used interchangeably throughout the text.

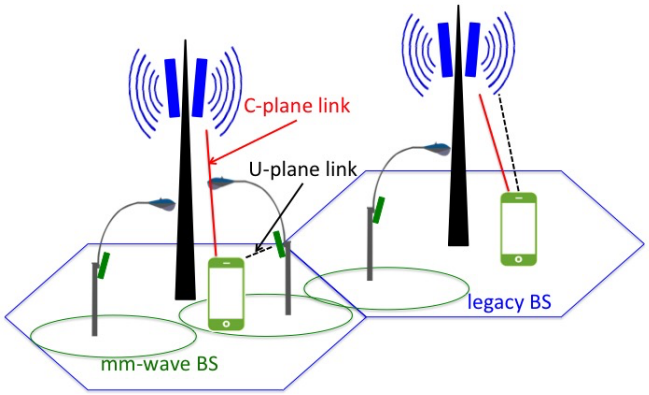

Fig. 1. Example of C-/U-plane split architecture in mm-wave Radio Access Networks.

the user plane (U-plane) and control plane (C-plane)[2]. While the former enables network controllers to centrally perform network operations, such as resource allocation, beam steering, etc. [6], the latter guarantees a full coverage by exchanging signaling messages with legacy BSs (typically macro cells) and provides ultra-high capacity channels by means of mm-wave small cells activated on-demand [7], as shown in Fig. 1. This solution has been recently considered within the MiWEBA[3] project and other EU-5GPPP project frameworks (e.g., MiwaveS[4], 5grEEn[5]).

While mm-wave transmissions pursue an innovative revolution of wireless access experience, access network facilities built on top of mm-wave technologies pose additional complexity in conventional network operations, e.g., the initial network access. Legacy network architectures, wherein synchronization signals are typically broadcast within the cell area to be sensed and demodulated by the mobile terminal, must be properly amended: the directional nature of mm-wave communications requires the transmitter and the receiver to be spatially aligned, and thus, a novel discovery process must be conceived. This process consists in a geographical scan of the cell area (performed by both transmitter and receiver), sweeping through all possible directions. Discovery processes inappropriately designed might incur in large delay in the user access, while negatively impacting handover procedures ([8]), as well as the user quality of service (QoS).

In this work we present a thorough study on smart cell discovery schemes properly formulated for mm-wave RAN architectures. Our analysis unveils a *novel fast and efficient cell discovery procedure* relying on the new architecture proposal. In particular, driving the initial search on the basis of the *user-location information* collected from the separate C-plane signaling, our solution outperforms the currently available discovery procedures by limiting the access delay. We derive

2. Although such a functional separation is not a novel concept in the network design, it has been recently introduced in the mobile cellular area. Beyond Cellular Green Generation (BCG[2]) [5] project within the GreenTouch Consortium (http://www.greentouch.org) has proposed the first complete architecture in 2011 for energy-saving purposes.

3. FP7-ICT EU-Japan Millimetre-Wave Evolution for Backhaul and Access (MiWEBA) project, http://www.miweba.eu.

4. FP7-ICT EU Beyond 2020 Heterogeneous Wireless Network with Millimeter Wave Small Cell Access and Backhauling (MiWaveS) project, http://www.miwaves.eu.

5. EIT-ICT Towards Green 5G Mobile Networks (5grEEn), http://wireless.kth.se/5green.

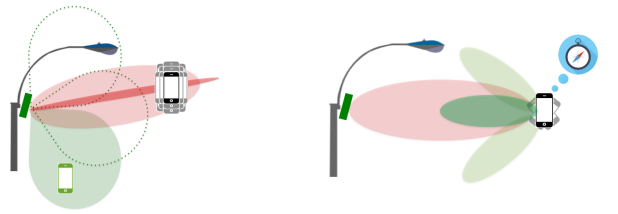

(a) Issues at cell side (b) Issues at mobile terminal side

Fig. 2. Directional cell discovery examples

an *accurate analytic model* taking into account directivity effects on both BS and MT side in order to compare the performance of different discovery algorithms. Analytical results are further supported by exhaustive simulations to assess the impact of uncertainty in the localization and propagation impairments in realistic scenarios. To the best of our knowledge, this is the first work investigating the *impact of obstacles* on the cell search process. Their effect, combined with the inaccuracy of the location information, can severely harm the cell discovery procedure. To deal with this issue, we propose a *geo-located context database* able to speed up the cellular attachment operations by storing and processing the information about the previous cell discovery attempts. The proposed framework enables the use of mm-wave communications in radio access networks by providing a fast and reliable cell discovery procedure in realistic network scenarios.

The article is organized as follows. We address the mm-wave initial *cell discovery* problem in Section 2. In Section 3, we discuss related works on directional cell discovery. We describe the proposed cell discovery algorithms and their analytic models in Section 4, while a thorough analysis of the numerical results is carried out in Section 5. The effect of the obstacles and the impact of the geo-located context database are described in Section 6. Finally, in Section 7, we discuss implementability issues of the proposed approaches. Section 8 ends the articles with some concluding remarks.

2 mm-Wave Initial Cell Discovery

A number of technical challenges come into play when applying a functional split. While legacy control functions assume that the service requests are collected and served by the same network entity, e.g., a base station, the functional separation abstracts the resource management functions providing a full network view to an independent entity. This requires richer user-context information in order to activate data network elements and, in turn, to approach the optimal utilization of system resources. The resource management becomes more complex, and thus, sophisticated resource allocation algorithms are required. Despite the functional split, some of the low level control functions cannot be delegated to a separated signaling connection with a different base station. Among these functions, the cell discovery process in mm-wave RAN is critical as it requires an initial directional scan that introduces an access delay.

Let us consider a simple cell discovery strategy consisting in sweeping through all possible antenna configurations while looking for a rendezvous between the mm-wave BS and the user. This process might take long time so that the

synchronization phase might be severely delayed. Current antenna technologies allow to use many different antenna configurations ([9]): *different beam widths* can be available, and, according to the beam width, many *different pointing directions* can be used [6].

The beam width selection has a significant impact on the discovery procedure. Large beam widths allow to scan faster over the surrounding space –fewer switches– but they can reach relatively close users. Vice versa, narrow beams can cover far away users, but they require a large number of antenna configuration changes to scan the entire space. As a consequence, the discovery procedure must undergo a trade-off between speed and range of the spatial exploration. The best mix clearly depends on available antenna configurations and users distribution. As shown in Fig. 2(a), the green wider beam allows to explore the space with a few configuration switches, however, it can cover only the green user. Indeed, the black user, farther away, cannot be reached with the green beam, but with a thinner beam such as the red one. In this case, several switches are needed to cover the same angular span so as to eventually find the user.

The context information is another relevant factor that should be considered. Within a split architectural paradigm, the cell discovery process might take advantage of acquiring information on mm-wave BSs and MTs. Generally speaking, the initial access procedure can be improved by richer information, e.g., terminal positions, channel gain predictions, user spatial distribution, antenna configurations successfully used in previous accesses, and so on. Ideally, if the context provided perfect information, mm-wave BS and user could directly discover and point each other with a narrow beam in one single step. In practice, inaccuracy is unavoidable, hence, context information can only be used to narrow down the search space and limit the searching time. Therefore, an advanced discovery algorithm is crucial to guide the search through the most likely successful configurations trying to minimize the number of attempts, even when only inaccurate context information can be obtained. For instance, Fig. 2(a) shows a black user affected by a unprecise position information. The choices of the discovery algorithm could range from selecting a very narrow and long range beam –so as to increase the gain toward the user's estimated position– to choosing a large beam width to be more robust against user location errors at the cost of a reduction in the user received power.

User's location plays a relevant role in speeding up the discovery when the context information is considered. Given the knowledge about the network deployment, the BS exploits user's location to point its beams towards the network area where a user is expected to be found. However, the same assumption cannot be made at user's side. Indeed, both position and orientation can only be estimated. In particular, the orientation is extremely critical as a small error can seriously impair every context information benefit, as shown in Fig. 2(b). A rotation of the MT antenna array can lead the receiver to focus towards wrong directions, due to a different reference system. Moreover, the limited energy and the limited computational power available at MT with respect to BS significantly reduces the complexity of implementable discovery algorithms. Therefore, it is reasonable to expect basic strategies to address directionality at user side. This is further supported by a number of theoretical and practical works considering greedy algorithms for steering the user beam based on sequential circular patterns until the mm-wave BS is successfully found ([10], [11], [12], [13]).

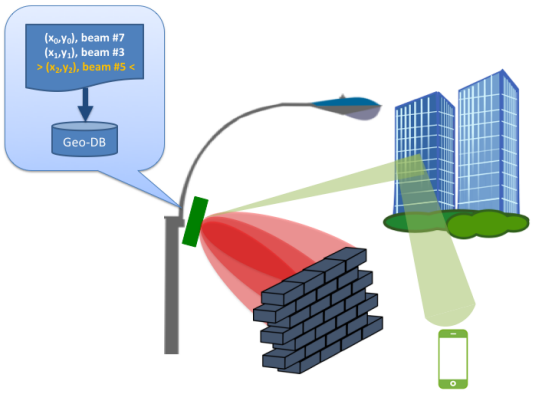

Fig. 3. Using geo-located context database to manage reflected paths.

Finally, due to unavoidable severe shadowing effects, obstacles (with static or quasi-static behavior) may strongly affect the cell discovery performance. On the one side, due to the high frequency, every object (i.e., human bodies, cars, trees, furniture, etc.) behaves as an opaque body, thus preventing signals from propagating through it. On the other side, the mm-wave propagation channel has a quasi-optical nature. Flat surfaces can be considered as mirrors [14], making reflected paths characterized by a non-negligible received signal strength, i.e., a viable alternative to the direct path, as supported by the experimental measurements conducted in [15].Hence, spatial scheduling solutions, if properly designed, may even reach hidden users and provide them ultra-capacity connectivity by leveraging reflected paths to overcome obstacle obstructions, as show in Fig. 3.

Please note that the use of reflected paths may reduce the efficiency of basic cell discovery algorithms relying on position information, as they typically assume the LOS beam availability. When the LOS beam is obstructed, the algorithm must search among other antenna configurations until synchronization operations can be successfully performed. This makes the initial cell discovery process even more challenging. Nevertheless, storing the history of past attempts per user position in a context database can substantially help to derive information on the most likely configurations for a specific location. Approaching the search with the previous successful antenna configuration, and then, in case of failure, switching to a smart discovery algorithm, could be a simple but effective solution that greatly reduces the discovery time. The management of this geo-located context database is an aspect that must be carefully investigated, as it can provide a remarkable speed-up to the cell discovery process in mm-wave RAN facilities, as already pointed out in other research areas [16].

In the rest of our work, we start considering an obstacle-free scenario wherein we propose smart discovery algo-

6. In this work, we assume a fixed transmission power for the mm-waves small cell deployment following the current standardization bodies (e.g., 3GPP or NGMN). However, our proposal could be easily extended to admit advanced power control schemes.

rithms. They provide advanced procedures to minimize the number of antenna configuration attempts in order to establish a connection with a signal power level sufficient to acquire the synchronization signal. After a complete dissertation, through an analytical and a numerical analysis of the obstacle-free case, we introduce obstacles in our scenarios. We discuss how context information about past successful attempts could be processed and used to further improve the overall system performance.

3 Related works

Mm-wave technologies rely on high-gain directional antennas. While they are playing a leading role in the design of future networks, their issues and challenges have been extensively studied in the past for ad-hoc wireless networks [17], where MAC protocols have been introduced to cope with the initial access problem. In [18], protocol details are provided with a focus on the association and discovery phase in short-coverage environments, whereas Ramanathan *et al.* present in [19] a complete framework for ad-hoc networks adopting directional antennas, pointing out technology challenges and off-the-shell solutions. A widely-accepted conclusion of all these works is that, while improving spatial reuse and extending the link range, directional communications exacerbate deafness and hidden terminal problems and increase the complexity of the neighboring discovery process. Thus, most of the research works tend to consider a control plane management performed by omnidirectional interfaces which orchestrates the beamforming operations [20] or to assume a blind spatial search to detect the user signal [21]. Interestingly enough, devices in Wireless Personal Area Networks (WPANs) are typically provided with omnidirectional sensing capabilities for neighboring discovery, whereas they can focus their beam towards incoming signals by using beam tracking algorithms, as shown in [22]. Tracking algorithms to avoid obstacles on the direct path are used as well, as illustrated in [23].

The evolution of Wi-Fi networks has blended together recent mm-wave technologies and advanced directional MAC protocols. A new standard, IEEE 802.11ad, also known as WiGig, has been proposed to boost the WLAN performance by increasing the overall spectral efficiency. In this standard, the cell discovery process leverages the information collected during a periodic beamforming training period. Several solutions have been proposed to improve the standard. A good solution is presented in [24] where Access Point (AP) beam parameters, such as its width, are optimally selected to reach every subset of surrounding users. Conversely, in the uplink context, the optimal directional beam information is analyzed in [25], where a novel MAC protocol selects the best direction found during a training period to beam towards a relay station whenever channel conditions degrade. The work in [26] presents a joint beam width selection and power allocation problem in order to maximize the overall network throughput in an mm-wave wireless network affected by deafness and misalignment impairments. Due to the huge complexity and the full topology awareness required by the optimal solution, the authors propose two standard compliant schemes which exploit directionality to maximize the reuse of available spectrum while imposing almost no computational load. Finally, [27] proposes an interesting work on smart beam steering algorithms applied to mm-wave wireless LAN. Specifically, the proposal exploits previous information to narrow down the sector search space while users move.

None of the presented prior works aims at facing cell discovery issues in cellular networks, although they paved the way for developing new protocols to handle the ever-increasing requirements of future cellular networks.

Recent researches have started investigating mm-waves as a promising technology to be adopted in 5G networks. Some of the first works in this direction are [8], [4], [28], and [29]. The authors in [8] show that a mismatch between the discoverable network area and mm-wave service coverage could occur, and it is detrimental to the cellular network operations. In [4], an analytical model for cellular coverage (and rate performance) is presented by means of distance-dependent Line-Of-Sight probability function. Based on such a model, the authors have proven that dense mm-wave networks can achieve much higher spectral efficiency w.r.t. conventional cellular networks, while providing considerable cellular coverage. However, transmission blockages and coverage discontinuity make the full mm-wave deployment far from being practically viable. In [28] and [29], we initially proposed fast cell discovery procedures leveraging context information and provided a very preliminary approach to deal with obstacles and reflected rays.

In [11], [30], the cell discovery procedure is addressed from a physical-layer perspective. Analysis and solutions are presented, however, the work focuses on acquiring channel synchronization, thus, it is somehow orthogonal to our proposal. Similarly, [31] unveils an effective strategy for transmitting the reference signals (RSs) used in the BS discovery process. The authors in [32] discuss MAC layer design issues for cellular networks, identifying challenges and solutions. In addition, they provide a model for the spatial search delay when semi-directional or fully-directional mm-wave antennas are considered. Although being an accurate model, it assumes that directional synchronization pilots are transmitted in a first phase to get BSs and MTs synchronized both in time and space. Then, a spatial search is carried out to get BSs' and MTs' antennas aligned. This two-step access procedure might further delay the discovery process, therefore, we apply an one-step procedure in our proposal. In [33], an evolution of the 3GPP standard for user association is presented by pointing out mm-wave challenges and, in particular, how to prevent connection losses. The authors propose two BS synchronization options: i) an omni-directional synchronization signal able to cover the entire cell area or ii) a sequence of narrow directional synchronization signals with fixed beam width, sequentially varying their directions. Conversely, in our work we analyze different sequences and combinations of beam widths and directions in order to shed light on the complexity of the cell discovery mechanisms and its delay implications.

An overview of iterative and exhaustive cell search schemes has been provided in [34], where also different algorithms have been compared. Very recently, in the work-in-progress paper [35], an approach based on context information and directivity of mobile antennas has been proposed.

With respect to the above literature, in this article we provide the following novel contributions:

- we propose smart cell discovery procedures relying on the C-/U-plane architectural split;
- we propose a mathematical formulation to estimate the probability of being discovered within a short time window by using cell discovery procedures;
- we introduce the use of mm-wave path reflections to avoid obstacles and reach hidden users;
- we propose and evaluate a context-based approach which, leveraging past access information, minimizes future search delays;
- we validate our approach by exhibiting outstanding results against basic search approaches in presence of obstacles, to the best of our knowledge, no advanced study has addressed this problem so far.

4 Obstacle-free Fast Cell Discovery

Upon joining the network, a new user starts seeking for the synchronization signal sent through a BS beam. At one extreme, if no context information is available, the BS (user) randomly selects a beam width and a pointing direction while probing around to spot potential users (BSs). Upon receiving a signal power level above the minimum detection threshold, the user reports channel information and starts the association process. Clearly, this scheme might result in a very long cell discovery time due to the randomness of the user's position and orientation. At the other extreme, assuming a perfect knowledge of user's position, user's orientation, and propagation environment, the BS and MT can readily compute the proper pairs $b_0 = (w_0^{BS}, d_0^{BS})$ (beam width, pointing direction) and $m_0 = (w_0^{MT}, d_0^{MT})$ to provide a sufficient signal power level to get reciprocally connected in one single attempt. This trivially minimizes the cell discovery time. The real condition is somehow between these two extremes: although not perfect, the information about the user position can significantly speed up the cell discovery procedure.

Note that, an optimal beam selection implies the knowledge of the path loss between the MT and the BS, which could be estimated by using channel models [2] or anchor-based prediction systems [36] with a given accuracy. However, for the sake of simplicity, given the statistical properties of such estimations, we can consider channel path loss and user location errors merged together in a unique equivalent location error.

If the user is not immediately detected with the initial beam b_0 due to the inaccuracy of the provided position, the discovery proceeds with other beams according to a given search sequence $b_1, ..., b_m$. Similarly, at MT side, the first beam m_0 is activated and, if no signal from the BS is detected, the other beams of the search sequence $m_1, ..., m_n$ are sequentially explored. As explained in Section 2, MT discovery algorithms are required to be lightweight and simple so that we can expect the MT's search sequence to be remarkably shorter than BS's one, $n < m$. Therefore, for each BS beam switch, the whole MT's search sequence is explored, scanning through its n beams. Upon completing the whole set of possible MT beams with no successful acknowledgment, the BS moves to the next beam and the MT's beam sequence exploration restarts. This process requires a BS beacon transmission at each MT switch, this implies a loose synchronization between MT and BS, which can be easily established through the legacy C-plane connection.

Only when an MT and a BS eventually activate two beams that allow them to point each other so as the BS beacon can be decoded at MT side, the cell discovery is concluded. This can be then confirmed by the user through a prompt message transmitted on the mm-wave interface, or through the legacy C-plane interface, which can notify the success to the BS. The best option is determined by the network architecture and the mm-wave MAC protocol, however, although being an interesting issue, it cannot be addressed in this work due to space limitation reasons. When the whole BS search sequence has been explored without a positive feedback, the user is marked as unreachable.

We consider a 2D environment (fixed elevation angle) [7] wherein devices are equipped with a steerable antenna, having a discrete set of beam widths W_{-3dB} and pointing directions D. The number of pointing directions with a beam width $w_{-3dB} \in W_{-3dB}$ is $N = 2\pi/w_{-3dB}$. Beam width and antenna gain are linked together by a Gaussian main lobe profile [37]:

$$G_{dB}(\phi,\theta) = 10log\left(\frac{16\pi}{6.76\cdot w^{\phi}_{-3dB}\cdot w^{\theta}_{-3dB}}\right) - 12\cdot\left(\frac{\phi}{w^{\phi}_{-3dB}}\right) - 12\cdot\left(\frac{\theta}{w^{\theta}_{-3dB}}\right) \quad (1)$$

where ϕ and θ are defined as offsets between the main lobe direction and the elevation angle and azimuth angle, correspondingly, while w^{ϕ}_{-3dB} and w^{θ}_{-3dB} are respectively elevation and azimuth half-power beam widths. Since we consider only azimuth angles, in the following $w^{\theta}_{-3dB} = w_{-3dB}$. The same antenna model is considered at both BS and MT side. However, since MT antennas are smaller and less sophisticated than BS antennas, we will consider a smaller number of available beams and a smaller maximum directivity at MT side.

We cast the cell discovery problem into a search time minimization problem wherein an mm-wave user and an mm-wave BS must find $i)$ the beam width $w_{-3dB} \in W_{-3dB}$, and $ii)$ the pointing direction $d \in D$ in order to provide the user with a sufficient signal power level to detect the presence of the mm-wave BS beacon, and thus, to synchronize. A cell discovery procedure must define the search sequences of beams $\mathbf{b} = b_0, ..., b_m$ (i.e., {beam width - direction} pairs) and $\mathbf{m} = m_0, ..., m_n$ to be sequentially activated by, respectively, the mm-wave BS and the mm-wave MT.

Clearly, as the way $\mathbf{b}$ and $\mathbf{m}$ are designed strongly determines the performance of the discovery procedure, in the same way their design is strongly influenced by device capabilities and the available context information. In the next section, we discuss several design solutions for $\mathbf{m}$ and $\mathbf{b}$. Then, in Section 4.2 we present an analytic model to predict the cell discovery time when using generic search sequences.

7. While this could be seen as a limitation of our approach, it helps to better explain the problem and make our analysis tractable. However, introducing the third dimension will only enlarge the set of eligible beam pairs keeping our model still valid.

4.1 Cell Discovery procedures

The sequences of explored beams $\mathbf{b}$ and $\mathbf{m}$ are the key-features to determine the performance of the mm-wave cell discovery phase. Several approaches can be designed with different complexity, depending on the available user-context information. In this section, we focus on algorithms based on MT position estimates, which are conveyed to the network through the separated C-plane during the initial service request. We start by analyzing MT approaches, then we move to the BS side.

iBWS: Considering the limited computational power at MT, the sequence $\mathbf{m}$ cannot be designed according to a sophisticated algorithm. A realistic solution cannot be much more complex than the sequential circular patterns that are commonly adopted in literature ([10], [11], [12], [13]). Our improved approach, called *initial BeamWidth Selection* (iBWS), considers the availability of a dynamic beam width selection provided by current mm-wave antenna technologies. This overcomes the fixed-beamwidth constraint of previous approaches, which are based on the *Sector Level Sweep* (SLS) phase of IEEE 802.11ad BF protocol.

The iBWS procedure processes the MT's location, selects the best combination of beam widths at both BS and MT side, and then informs both devices through the separated C-plane connection. The selection is based on the estimated distance between BS and MT. This allows to increase the beam width when users are close to the BS, thus reducing the number of steps required to sweep through the surrounding area at both sides of the directional link. Compared with the SLS approach, which forces the use of the narrowest MT beam for any connection attempts, iBWS allows to save a remarkable number of switches when MTs are not at the cell edge.

Once the MT's location allows to estimate the overall BS-MT pathloss, the iBWS procedure must determine each individual tx and rx antenna gains. We consider the following three strategies: among the beam width combinations that allow to establish a connection, the selection considers

- *Wide BS - Narrow MT*: the one with the largest beam width at BS side;
- *Narrow BS - Wide MT*: the one with the largest beam width at MT side;
- *Balanced*: the one with the minimum difference between BS and MT beam width.

In addition, the width set at MT side, among those available, is the one just narrower than the selection outcome. This allows to mitigated possible coverage problems due to a wrong beam width selection caused by large location errors or obstacles.

iBWS provides the initial widths w_0^{BS} and w_0^{MT} of b_0 and m_0 beams, whereas the selection of their directions and those of the next explored beams is delegated to the cell discovery procedures that generate $\mathbf{b}$ and $\mathbf{m}$. At the MT side, beams in $\mathbf{m}$ are those of a circular sweep that starts from a random direction and considers only $\frac{2\pi}{w_0^{MT}}$ steps. As for the BS, the discovery procedures to generate $\mathbf{b}$ can be much more complicated, therefore they are individually described in the next paragraphs.

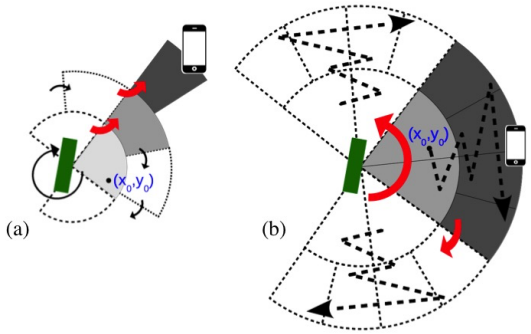

Fig. 4. Illustration of (a) Dynamic SLS and (b) Enhanced Discovery Procedure. Estimated user location is (x_0, y_0).

gSLS: A first procedure to populate $\mathbf{s}$ consists in a straightforward extension of the SLS phase of IEEE 802.11ad BF protocol. It ignores iBWS and considers a fixed beam width, set to the narrowest available value in order to preserve the largest coverage. The procedure starts by configuring the beam parameters pair (w_{MIN}^{BS}, d_0) (beam width and pointing direction) that cover the nominal user position (x, y), then, it proceeds to circularly sweep through adjacent beams until the whole circle has been explored. Users that cannot be discovered by this procedure are defined as unreachable.

D-SLS: As a first improvement over gSLS, we apply a search paradigm that dynamically adapts beam widths, called *Dynamic SLS* (D-SLS, see Fig.4(a)). The search starts considering the beam (w_0^{BS}, d_0), with the width w_0^{BS} set by the iBWS strategy and direction d_0 such that the user at (x, y) can be reached. If the user is not detected, the mm-wave BS sequentially scans around through every direction, keeping the same beam width w_0^{BS}. If no user is still found, the mm-wave BS restarts the circular sweep with a reduced beam width. The next circular scan will cover a larger area and will consist of a larger number of attemps. The procedure repeats until every combination of beam width and pointing direction is explored. The rationale behind D-SLS is the idea of exploring the close-by neighborhood through wide beams thereby allowing to reach nearby users faster than SLS.

EDP: In order to exploit the context information in a smarter way, we propose an enhanced version of the D-SLS procedure, named *Enhanced Discovery Procedure* (EDP) (Fig.4(b)). As in the previous approach, when a new user joins the network, the serving BS quickly computes the correct beam width and pointing direction, (w_0^{BS}, d_0), to properly beam the user based on the estimated position. If the position is not accurate, the user might not be spotted, thus, the BS scans the surrounding environment relying on n circular sectors, each $(2\pi/n)$-radian wide. The first selected sector, r, corresponds to the area containing the estimated (inaccurate) position of the user. To overcome the inaccuracy of the position, the BS starts exploring the sector r through beams with a fixed width w_0 and directions adjacent to d_0. During this exploration the BS considers alternate clockwise and counter-clockwise beam directions. If no user is reached, the BS narrows the beam width, points the beam again towards the estimated user position, and similarly explores adjacent beam directions within the

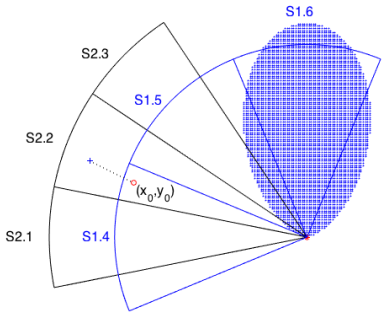

Fig. 5. Beam footprint and model sector approximation. The dashed region is the coverage footprint approximated via sector S1.6. The red dot is user's nominal position, while the blue cross is its real position.

sector. After completing the scan of the first sector without any user connection establishment, the same scan iteration is repeated for each of the other adjacent $n-1$ sectors, alternating clockwise and counter-clockwise sectors. In each sector, the exploration starts from the relative {beam width, pointing direction} pair corresponding to (w_0^{BS}, d_0) in r. The process ends when the UE has been detected or when all n sectors have been scanned without any user connection. Note that if we are in case of many and narrow sectors and the nominal user's position is close to the BS, the first wide beams used to explore a sector could be the same first beams of the exploration of adjacent sectors. In this case, repeated beams are skipped, and the sector exploration starts directly from the narrower beams.

The Enhanced Discovery Procedure aims at providing a good trade-off between two opposite strategies: i) first scanning large azimuthal angles and then extending the range by narrowing the beam, or ii) first exploring narrow azimuthal angles until the maximum range is reached and then changing pointing direction. As shown in the next section, the most convenient strategy depends on UE distribution statistics and position accuracy.

4.2 Stochastic model

In order to model the mm-wave initial access, we consider a scenario where users' nominal positions (e.g., the one indicated by the localization system) are distributed according to a bidimensional density function f_{XY} in a square area of side length l. Each user nominal position (x, y) is affected by a localization error described by a symmetric and independent bivariate normal distribution characterized by parameter σ and centered in (x, y)[8], while user orientation is randomly chosen. Users are dropped in the obstacle-free square area and the mm-wave BS is placed in the middle.

As shown in the sector $S1.6$ of Fig. 5, we consider the coverage footprint of a pair of beams selected by MT and BS, that is, the area surrounding the BS where an MT can correctly decode BS signals when the BS beam is active and the MT beam is pointing towards the BS. We approximate it with a circular sector described by three parameters: radius, angular width, and pointing direction. We use the half-power beam width w_{3dB} of the BS beam as sector *angular width* and, as sector *pointing direction*, the same as of the BS beam, $p = k \cdot w_{3dB}$, with $k = 0, .., \frac{2\pi}{w_{3dB}} - 1$. Finally, as sector *radius*, we set the maximum distance, scaled by a factor η, at which user and BS can connect if both MT and BS beams are perfectly aligned. Basically, we consider the combined maximum gain of the beams selected at both BS and MT. Our design introduces two approximations: i) while the real footprints of adjacent beams slightly overlap, sectors with a given width can cover 2π radians without overlapping, ii) while the model considers a perfect MT-BS alignment, user beam directions are fixed, depending on user's orientation. Therefore, MT and BS beams could never be perfectly aligned during the MT scan. This reduces the maximum coverage distance, which we model with the factor η. Nevertheless, these approximations allow to greatly simplify the model without substantially impairing its accuracy, as shown in the next section where model results are validated against simulated ones.

Given the user's nominal position (x, y), first, the iBWS strategy ρ selects a pair of beam widths, then, BS and MT select two beam pointing directions in such a way that the BS beam can potentially cover (x, y), provided the MT beam points towards the BS. In the model, this translates into determining the circular sector, with direction, width and radius defined as above, that includes (x, y). This is a straightforward operation.

If this first connection attempt fails due to the MT's location and orientation errors, the process resorts to the two search sequences $\mathbf{b}$ and $\mathbf{m}$, respectively at BS and BT side, generated according to the specific discovery procedure and the iBWS strategy ρ. We can separately analyze how the sequences have been modeled, starting from the BS side.

If we label every possible BS beam configuration (w_{3dB}, p) with an identification number, we obtain that each BS cell discovery procedure (gSLS, D-SLS, EDP, etc.), α, provided with the initial location (x, y), defines a numerical sequence $\mathbf{b} = \mathbf{b}\{\alpha, \rho, (x, y)\}$ of beam identifiers. The n-th element of $\mathbf{b}$ indicates the circular sector corresponding to the BS beam selected at the n-th step of the search process at BS side, which is fully described by the MT antenna gain resulting from the iBWS strategy ρ. If the MT is located within this sector, the connection will be established using the corresponding BS beam and one of the MT beams of the MT sequence $\mathbf{m}$.

In order to assess the performance of a cell discovery algorithm α (which depends on iBWS procedure ρ), we are interested in computing the probability of connection establishment at step n of the BS search sequence. We name $p_{BS,n}^{\alpha,\rho}$ the probability mass function (pmf) at BS. The pmf $p_{BS,n}^{\alpha,\rho}$ can be computed considering that an MT in the coverage footprint defined by the BS beam b_n will get connected during the MT scan before the BS moves to the next beam. Therefore, it can be expressed as follows:

$$p_{BS,n}^{\alpha,\rho} = \iint p_{BS,n}^{\alpha,\rho}(x, y) f_{XY}(x, y) \mathrm{d}x\mathrm{d}y, \qquad (2)$$

where $p_{BS,n}^{\alpha,\rho}(x, y)$ is the conditioned probability of connection at the n-th step of algorithm α, given the user's nominal location (x, y). We can express the conditioned probability as:

$$p_{BS,n}^{\alpha,\rho}(x, y) = \iint_{A_n\{\alpha,\rho,(x,y)\}} \mathcal{N}(x, y; x, y, \sigma) \mathrm{d}x\mathrm{d}y \qquad (3)$$

8. We rely on the modelization of the localization error commonly applied into standard GPS systems [38].

where the normal distribution of the location error $\mathcal{N}$ is described by the parameter σ, and shifted to (x, y). Depending on the algorithm α and iBWS procedure ρ, $A_n = A_n\{\alpha, \rho, (x, y)\}$ is the area obtained as the difference between the area of sector b_n and the area of the overlapping sectors with a smaller radius (i.e., larger width than b_n), which have been already explored in the sequence $\{b_0..b_{n-1}\}$. If no overlapping sector belongs to the sequence, A_n corresponds to the whole area of sector b_n.

In Fig. 5, sector $S1.5$ overlaps only with sector $S2.3$, while sector $S2.2$ has two adjacent overlapping sectors, $S1.4$ and $S1.5$. When $b_n = S2.2$ and only $S1.5$ is in $\{b_0..b_{n-1}\}$, A_n splits into the annulus sector determined by $S2.2$ and $S1.5$, and the remaining circular sector obtained by subtracting the overlapping area of $S2.2$ and $S1.5$ from the $S2.2$ area. From the definition of A_n derives that overlapping sectors are always wider than the reference sectors, this means that the case in which more than two adjacent sectors overlap with a narrower sector does not exist.

Finally, the way A_n is computed is related to the probability of connection at step n. Indeed, in order to have a successful discovery at step n, the user must lie in a region of the sector b_n covered by none of the sectors $b_t, t \in [0, n-1]$, otherwise, the BS beacon would have been already detected before step n. The computation of A_n is greatly simplified by the removal of the overlap among sectors with the same width.

As for the MT side, although the sequential circular exploration defined by $\mathbf{m}$ does not depend on α, the overall number of steps carried out at MT is strongly influenced by the number of wrong BS beams previously tested. Indeed, for each BS beam, a full circular sweep is performed by the MT. The number of steps MT requires to complete a full circular sweep, M, depends on both user location (x, y) and iBWS strategy ρ, i.e., $M_\rho(x, y) = \frac{2\pi}{w_0^{MT}(\rho, x, y)}$. In addition, once initially defined, the MT beam width w_0^{MT} remains constant, therefore, M does not change during the whole discovery. This allows us to use the BS pmf to compute the probabilities at MT side, indeed, the conditioned probability of connection at the m-th MT step, given the user's nominal location (x, y), can be computed as:

$$p^{\alpha,\rho}_{MT,m}(x, y) = \frac{1}{M_\rho(x, y)} p^{\alpha,\rho}_{BS,\left\lfloor \frac{m}{M_\rho(x,y)} \right\rfloor}(x, y) \qquad (4)$$

where we can note that once the discovery probability at the corresponding BS step $\left(\left\lfloor \frac{n}{M_\rho(x,y)} \right\rfloor\right)$ is computed, the probability of connection in one of the steps of the MT sweep is uniform and equal to $\frac{1}{M_\rho(x,y)}$. The unconditioned probability $p^{\alpha,\rho}_{MT,m}$ can be finally computed in a way similar to the one shown in Eq. (2).

5 Numerical Evaluation

In this section, we assess the cell discovery performance of the proposed algorithms by means of numerical simulations carried out by an ad-hoc MATLAB® simulator. If not stated differently, we consider the following scenario. We place one mm-wave BS in the middle of a 450 x 350m area, while 1000 users are dropped according to different distributions, as described later, while their orientation is randomly chosen. We model the user-location uncertainty by considering the real user position distributed as a symmetric and independent bivariate normal distribution centered in the nominal position with parameter $\sigma_x = \sigma_y = \sigma$. We consider a location error $\epsilon = 3\sigma$. The antenna gain is modeled with a Gaussian main lobe profile described in Eq. (1), while the path loss model used for the transmission is defined as follows:

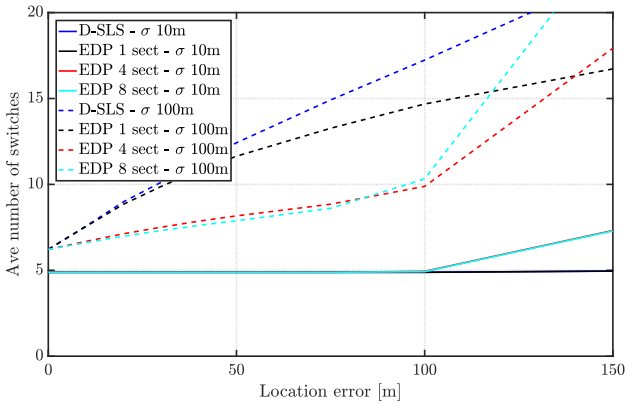

Fig. 6. Performance evaluation for different BS discovery procedures and σ of the user normal distribution.

$$\mathrm{P}(l) = 82.02 + k \cdot 10 \log\left(\frac{l}{l_0}\right) \qquad (5)$$

where reference distance l_0 is 5 meters and the propagation factor k is 2.36, if the distance between the transmitter and the receiver is larger than the reference distance, or 2.00 otherwise. For more details, e.g., fading and other channel properties, we refer the reader to [37]. The minimum signal level for primary synchronization signal (PSS) acquisition, $Th = -73dBm$, is directly derived from the empirical measurements presented in [30], where a Signal-to-Noise-Ratio (SNR) greater than 10dB has been experimentally confirmed. The BS transmitting power is set to $P_t = 30dBm$. The smallest configurable beam width at BS side is 3 degrees, which means the availability of non-overlapping beams pointing towards 120 directions. Larger beam widths are obtained by proportionally reducing the number of directions to $72, 36, 24, 12, 8, 4, 3$, and 1 for a total number of 280 antenna configurations available at BS side. As for MT side, we consider a more limited hardware, thus a reduced set of pointing directions. Namely, $12, 8, 4, 3$, and 1 possible equispaced beams to cover 2π radians. Finally, if not stated differently, we measure the cell discovery time in terms of antenna configuration switches at MT side. This is directly related to the cell discovery time according to the antenna hardware specifications. In the following, we analyze the performance of the context-based algorithms proposed in Section 4.1 varying the accuracy level of the MT's location information. We start by investigating the behavior of BS discovery procedures, then we proceed to consider the effect of different iBWS strategies.

Context: Geographical Position Accuracy

Fig. 6 shows the average rendezvous time, in terms of number of antenna configuration switches at user side, when the location accuracy varies and users are normally distributed

over the rectangular area with different standard deviations σ. The figure shows curves for two BS algorithms: D-SLS, and EDP. For the EDP algorithm, three curves are plotted varying the number of sectors n from 1 to 8. At user side, we assume SLS is used for this test: MTs performs the circular search by always selecting the narrowest beam width. Due to the smarter use of the user location information, D-SLS and EDP algorithms outperforms gSLS, which takes in average about 500 MT switches respectively to establish a connection. Focusing on the set of curves of the $\sigma = 100m$ scenario, we can note that EDP generally outperforms D-SLS, however results strongly depend on the location error. If the location error is small, the discovery procedures achieve a similar performance. When the provided MT's position is affected by a larger error, the gap is more evident. Indeed, when the location error is small, the user can be reached by the same beam or by beams adjacent to the one used to cover the nominal position. Therefore, even simple discovery procedures can achieve a very good performance. Instead, when the nominal and the real locations are far apart, a larger set of beam alternatives must be explored, therefore a smart discovery process makes the difference.

A further aspect to note in Fig. 6 is that increasing the number of EDP sectors allows to reduce the number of required step when the location error is small, however the number of step sharply increases when more sectors are used and the location error is large. Indeed, when the error increases, the higher error sensitivity of narrower sectors negatively impacts on EDP performance: the algorithm gets caught in a deep exploration of a sector that could be wrong due to the position inaccuracy. This effect impacts the relative performance of D-SLS and EDP as well: further increasing the location error beyond the values reported in the figure leads the D-SLS and EDP curves to cross. For those error values, the better context exploitation of EDP is detrimental, because the collected information is not representative of the real context. It is somehow a blurry view of the surrounding environment. This means that a discovery procedure not strongly based on the context, like D-SLS, can achieve a better performance as it is less misled.

We conclude the analysis of Fig. 6 with a comment on the set of curves of the $\sigma = 10m$ scenario. We can note that the number of required switches is remarkably smaller than in the previous scenario. Indeed, when users are close to the BS, they can be easily found by using very wide BS beams, thus reducing the number of steps to fully explore the surrounding area. In this case, actually any discovery algorithm can achieve a good performance.

Impact of the iBWS strategy

The impact of iBWS strategies on the discovery procedure consists in shifting antenna directivity from MT side (iBWS Wide BS - Narrow MT) to BS side (iBWS Narrow BS - Wide MT), to a similar directivity at both sides (iBWS balanced). The location error value influences the performance of each iBWS strategy, which in turn influences the efficiency of the selected BS discovery procedure. We have investigated on different combinations of these techniques and the results are shown in Fig. 7.

Fig. 7(a) shows the average number of required switches applying different iBWS strategies to D-SLS and EDP with

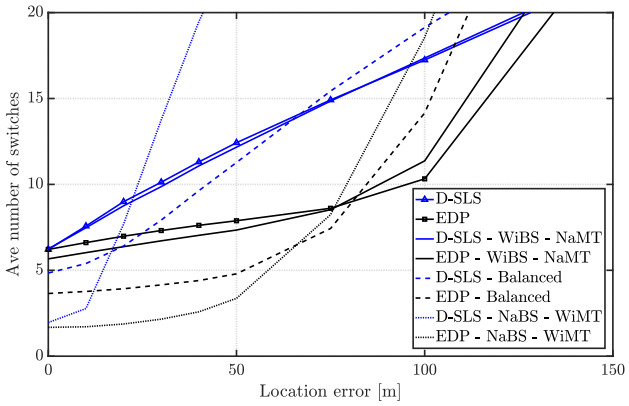

(a) Population of 1000 users normally distributed with $\sigma = 100$.

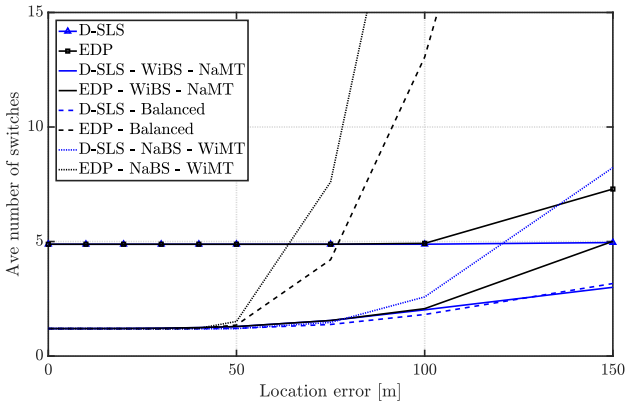

(b) Population of 1000 users normally distributed with $\sigma = 10$.

Fig. 7. Performance evaluation for different iBWS strategies and user distributions

different location errors, when users are normally distributed with $\sigma = 100m$. For sake of comparison, two curves show the D-SLS and EDP performance without iBWS (i.e., MT uses SLS) as well. The blue curves indicate D-SLS results, while black ones refer to EDP.

Focusing first on D-SLS results, we note that the performance of the "Wide BS - Narrow MT" strategy is very similar to the one without iBWS, in which SLS at MT side only considers narrowest beams. Indeed, shifting the high directivity to the MT side leads to a beam width selection that is similar to that provided by SLS. Vice versa, the "Narrow BS - Wide MT" strategy has a remarkably different behavior. Indeed, when the location error is small, the number of required switches is greatly reduced, while as the error increases, the strategy becomes less and less convenient. For very large location errors, it is even detrimental to the discovery. This behavior can be explained by observing that this strategy tends to select wide beams at the MT, which will complete a circular sweep in very few steps. In addition, when the location error is small, the BS can ideally reach the user in a single step. The combined result of this two effects is that the MT requires very few switches to find the beam pointing towards the BS and get connected. On the other side, the small MT directivity puts the user virtually far away from the BS, i.e., the link budget must be mainly covered by the BS antenna, which has to select narrow beams. This makes the performance of D-SLS more sensitive to location errors, as shown in Fig. 6. This is the reason why the curve sharply increases when the

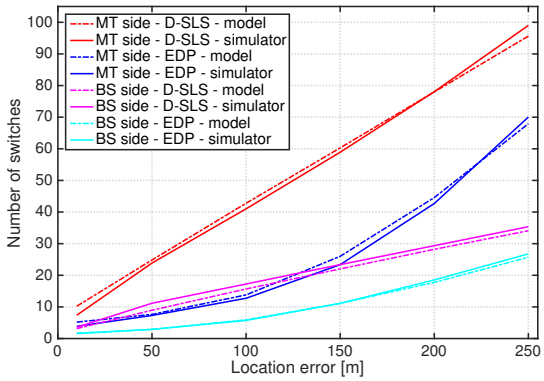

Fig. 8. Comparison between analytical and simulated results on the average number of BS and MT switches for different location error values.

location error increases. Finally, the "Balanced" strategy has an intermediate behavior, as expected.

Moving to EDP results, we can state that the trend shown by the black curves can still be explained by the same line of reasoning followed in the D-SLS case. In addition, it is again evident how EDP generally outperforms D-SLS when the location error is small, while it degrades and becomes less and less convenient with larger errors.

Fig. 7(b) shows the very same scenario as in Fig. 7(a), with the only difference that the normal distribution that describes user locations has $\sigma = 10$. We can note how the use of iBWS strategies is very effective when the location error is small, leading the discovery phase to be very close to the remarkable result of establishing a BS-MT connection at the first attempt. This is mainly due to the proximity of the users, which allows to select at both BS and MT side an antenna pattern that most likely is omni-directional. When the error increases, the performance clearly worsens. In particular, the "Narrow BS - Wide MT" strategy tends to suffer more the worse location accuracy for the same above-mentioned reasons. One last thing that can be noticed is that EDP tends to perform worse than D-SLS at large location errors, but smaller than in the previous figure. This could be explained by considering that, when users are close to the BS as in this case, it is more convenient to favor an angular space exploration than a radial one, as happens in D-SLS.

Model quality assessment

In order to assess the level of approximation introduced by the model described in Section 4.2, we have compared the performance predicted by the analytic model with those empirically obtained with the simulator. We have considered the same realistic scenarios described above, however, for sake of brevity, we show results only for the case of users dropped according to a uniform random distribution, EDP and D-SLS BS discovery procedures, and "Wide BS - Narrow MT" iBWS strategy. Nevertheless, we want to remark that our proposed model works with any other user distributions and discovery procedures, so as similar results can be obtained and similar conclusions can be drawn.

Fig. 8 plots the average number of BS and MT switches needed to establish a connection in case of different location errors, computed through the pmfs derived in Section 4.2. The figure confirms the high accuracy of the model by showing a very small gap between analytical and simulated values for every practical location error value. As expected, it also shows that the number of required steps increases as the error increases.

6 Dealing with Obstacles

Real environments are characterized by objects that can lie between mm-wave transmitters and receivers causing severe signal attenuations. These objects can be static (trees, buildings, etc.) or nomadic obstacles (human bodies, vehicles, etc.). While the effect of mobile obstacles can be modeled as a random fading and, thus, addressed by physical layer solutions, fixed obstacles systematically drop the signal and must be avoided from an upper layer perspective.

Since the propagation of mm-waves through obstacles is practically unfeasible, the only viable solution is to deviate from a LOS path and turn around the obstacle. Resorting to deviated paths is particularly efficient with mm-waves because of the good reflectivity of walls at high frequencies [15]. Considering surfaces as quasi-perfect mirrors, when a user is not reachable via a direct beam the cell search algorithm can leverage ray reflections to provide the user with a minimum level of power. In the ideal scenario where the network is perfectly aware of users' locations and obstacles' shapes and positions, the cell discovery procedure could promptly compute beamforming parameters at BS and MT side for the best reflected path. However, a detailed map of the area may be unpractical to retrieve, or it may require time-consuming in-field surveys. A more practical approach is based on geo-located context Data Bases (DBs).

Obstacles may notably delay the cell discovery process, in particular when advanced discovery algorithms are implemented. Indeed, algorithms are designed to focus BS beams around the nominal user's position, assuming LOS conditions. However, the reflected path can substantially deviate from the LOS path, thus a long sequence of candidate BS beams could be explored before finding the one covering the user. At MT side, the impact is less relevant. Indeed, the sequential beam scanning usually starts from a random position and is less influenced by LOS path deviations. A further effect of deviations is that they lengthen paths, thus

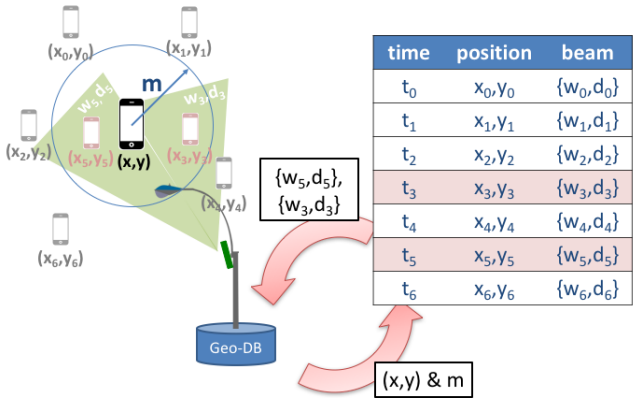

Fig. 9. Example of range m setup in the geo-located context database.

increasing path losses, which require narrower beams to be covered.

The effect of obstacles can be summarized as an error shift between the direct BS beam covering the nominal user's position and the correct BS beam used to reach the user in the real position. This shift presents similar features as the position error. Nevertheless, it is deterministic, allowing the algorithm, once the user is discovered, to store the correct beamforming configuration in the DB in terms of $\{(x, y), w, d\}$ tuples, where user's position (x, y) is bonded to BS beam parameters (beam width w and beam direction d). This approach takes advantage of past attempts, speeding up the discovery process when a new user service request comes from a "known" position (or close to that). Considering the huge impact that even a small user orientation error can have on the stored MT beam and the random start of BS search sequences, only BS beam information will be included in the DB.

The use of the DB information, however, is not straightforward: Here we carefully address the definition of "closeness" to a position associated to a DB entry. To this aim, we introduce a range m. Given a new user requesting access from a nominal position $p = (x', y')$, m indicates the maximum distance from p within which candidate entries can be considered in the DB, as shown in Fig. 9. The discovery phase tests all BS beam configurations of valid entries, which are sorted based on their distance from p. Note that, although multiple entries can suggest the same beam configuration, each beam configuration is activated only once, at the closest entry. If the user is not found using DB information, the search proceeds by activating one of the algorithms proposed in Section 4.1.

The range m is strictly related to the spatial correlation of the scenario with obstacles. If m is very small, the DB information may be underutilized. Only new mobile terminals placed very close to a known position can benefit of past attempts, even if the same beam configuration could be used for farther users as well. Vice versa, very large ranges may introduce misleading information. Indeed, the beam configurations that can cover very far-away positions are in general considerably different, therefore relying on "far" DB entries will likely produce unsuccessful attempts. In addition, a further source of spatial incoherence is the obstacle shadowing effect, which can change the successful beam configuration even for relatively close positions. Therefore, a good trade-off for designing m must be investigated. We discuss these issues and provide a numerical evaluation in the next section.

6.1 Performance evaluation

We carried out an exhaustive simulation campaign to evaluate the impact of the geo-located context DB in scenarios with obstacles. Numerical results are obtained with our MATLAB simulator considering the above-mentioned scenarios (please refer to Section 5), unless differently specified.

A $450m$ x $350m$ deployment area is characterized by $20m$ x $20m$ square obstacles uniformly dropped. We consider obstacles as opaque bodies with reflecting edges, we assume the area boundary reflecting as well. Since we investigate a simplified 2D scenario, ground reflections are statistically included in the propagation model in terms of random fading, i.e., they are not considered as possible reflected paths to reach MTs.

While the propagation model for LOS paths is the same as in Section 5, we model the path loss of reflected paths (by approximating it to the first and unique reflection) with the following equation:

$$\mathrm{P}_R = 82.02 + k \cdot 10 \log \left(\frac{l_r}{l_0} \right) + R + F \qquad (6)$$

where the reference distance l_0 is 5 meters and k is 2.36, if the distance between the transmitter and the receiver is longer than the reference distance, or 2.00 otherwise. Reflection losses are summarized by:

$$R = 20 \log \left(\tfrac{\sin\theta - \sqrt{B}}{sin\theta + \sqrt{B}} \right), \; B = \epsilon - \cos^2\theta;$$
$$F = \tfrac{-80}{\ln 10} \left(\tfrac{\pi\sigma \sin\theta}{\lambda} \right)^2.$$

We consider ϵ and σ as roughness and reflection coefficients of the material (namely, $\sigma = 0.2mm$ and $\epsilon = 4 + 0.2j$ [37]), while θ and l_r as the reflection angle and the length of the reflected path, respectively.

In Fig. 10 we first investigate the impact of the variation of the number of sectors n (or, equivalently, the sector width $2\pi/n$) on the performance of EDP algorithm in a scenario where the DB is not available. The figure indicates the average number of antenna configuration switches before a connection is established using EDP, in case of four different location error values. Results of D-SLS algorithm are reported as well for the sake of comparison. We consider a different iBWS strategy in each figure.

In Fig. 10(a), where "Wide BS - Narrow MT" is applied, we can see a remarkable delay decrease when the number of sectors goes from 1 to 5, then the improvement dramatically reduces further increasing the number of sectors. Vice versa, in Fig. 10(b), where "Narrow BS - Wide MT" is applied, the number of switches, which is far smaller than in Fig. 10(a), increases with the number of EDP sectors. In the first case, BS uses large beam widths, therefore a few and wide EDP sectors increase the rendezvous time because of the delayed exploration of areas far from the BS, i.e., more switches are needed to activate narrow beams able to cover longer reflected paths. In the second case, the iBWS strategy brings the BS to start the discovery from narrow beams, thus the exploration requires few steps to reach the end of sector, where very narrow beam are activated enabling reflected paths. Differently from the previous case, resorting to narrow sectors contributes more to increase the sensitivity to location errors due to the higher angular-selectivity than push the exploration to quickly activate narrower beams, which are already narrow. Therefore, the overall number of required switches increase. When the number of sectors excessively increases, large location errors produce an adverse effect and the finer context exploitation of the EDP algorithm is overcome by the sensitivity to location errors.

In addition to the above-mentioned far-exploration vs location-error-sensitivity trade-off, a further aspect impacts on the performance and it is more evident in Fig.10(c), where "Balanced" iBWS strategy is applied. If the EDP sector width is narrower than the BS beam width with which the discovery starts, the exploration of the next EDP sector

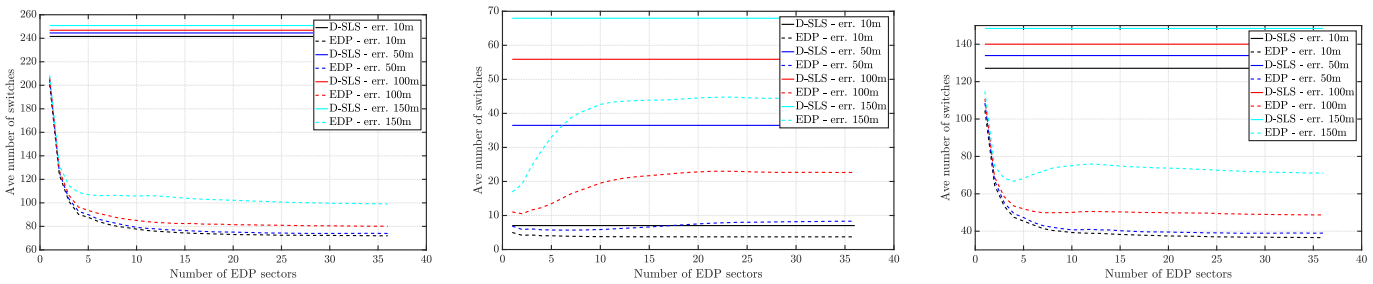

(a) "Wide BS - Narrow MT" iBWS strategy (b) "Narrow BS - Wide MT" iBWS strategy (c) "Balanced" iBWS strategy

Fig. 10. Performance comparison of D-SLS and EDP algorithms at different location error values when varying the number of EDP sectors.

should start from the same wide initial BS beam. However, the activation of a beam is never repeated in EDP search sequences. Therefore, since the initial BS beam is the same, the exploration of the next sector will start directly from narrower beams. The first wide beam will be skipped in the next sectors. This is true not only for the first beam of the EDP sector exploration, but also for every other beam previously activated. The final effect is that, if BS beams are sufficiently wide, narrower sectors lead to quickly activate only narrow beams before moving to another sector. This favors the discovery of reflected paths which are characterized by high path losses. This behavior is the cause of the second bend of the curves in Fig. 10(c)

A final consideration on the curves in Fig. 10 is that the selection of narrow MT beams for the circular sweep leads to discovery algorithms more sensitive to location errors. This is well shown by the increasing gap among the curves at different location errors in the three figures, both for EDP and for D-SLS algorithms. Therefore, considering the overall number of required switches as well, equipping MTs with less sophisticated antennas with limited directivity and leaving smart and sophisticated approaches at BS side definitively appears to be a promising design choice for the mm-wave initial cell discovery. This is the reason why in the following we fix the iBWS strategy to "Narrow BS - Wide MT" and evaluate the discovery time for different BS discovery procedures.

Considering now the introduction of the DB, Fig. 11 shows the performance in terms of number of switches MT requires to get connected, for different values of user location error and different numbers of obstacles dropped into the area. The x-axis of the plots shows the range of parameter m used to process DB entries and the value $m = 0$ indicates the DB is not used.

In Fig. 11(a), wherein a small location error of $10m$ is assumed, the presence of obstacles increases the number of required switches. Indeed, a BS beam directed to the nominal user's location cannot reach the user at his real position. This triggers an antenna configuration search. Clearly, more obstacles lead to a higher average number of antenna switches needed to establish a connection. Indeed, augmenting the number of obstacles directly increases the probability that the LOS beam cannot cover the mobile terminal. In addition, more obstacles make the difference between the direct beam and the covering beam larger, thus, the search for a new antenna configuration longer. The effect of the DB is to avoid this search after the first successful access. Accordingly, the figure shows how the improvement obtained by using the DB information is larger when more obstacles are dropped into the area.

A different scenario is evaluated in Fig. 11(b), where a large location error of $80m$ is considered. However, the advantages of using the DB information are still evident, the performance gain is even greater. A first aspect to note is that, as expected, the number of required switches is much higher than in the case of small location error, due to the combined effect of obstacles and location error. We can also note that the impact of the DB is more evident when D-SLS is used. Indeed, since the D-SLS is less efficient than EDP, finding a user with the DB information allows to save a larger number of beam switches.

Finally, an interesting behavior of emerges in Fig. 11. Fig. 11(a) shows a marked minimum point when the DB range increases. Indeed, a too small range prevents the full exploitation of the DB: only users very close to a DB entry can access the DB, even if the same information could be useful for more distant users. Vice versa, when the range is too big, many beams suggested by the DB will be uncorrelated with the user location, thus leading to a wastage of unsuccessful beamforming attempts. This behavior is less evident, but still present, in Fig. 11(b), where the large location error allows to better exploit beams in a large DB range. This aspect will become clearer after the analysis of the DB behavior in the next paragraphs.

The impact of the range m on the performance can be understood from Fig. 12 and Fig. 13. Fig. 12 shows the average number of antenna configurations available in the DB for users that eventually connect to the BS using only DB information. It analyzes the dependence of this number on the range m in scenarios with different numbers of dropped obstacles and location error intensities. As expected, it clearly shows that a larger DB range provides more configurations to be tested for incoming users. Note that D-SLS and EDP values are the same. Since both algorithms get the same successful beam, the DB will be populated with the same content as well.

In addition, Fig. 12 shows that applying the geo-located DB in scenarios with higher location errors produces larger sets of candidate beam configurations. Indeed, due to the higher location error, a certain DB range, which selects DB entries according to their nominal positions, will correspond to a sparser set of real positions. Those real positions will

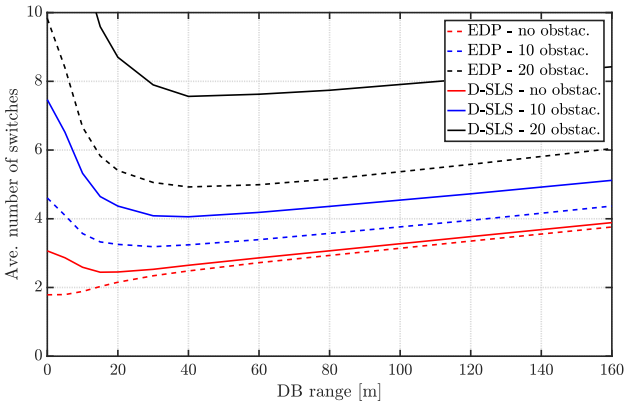

(a) $10m$ location error.

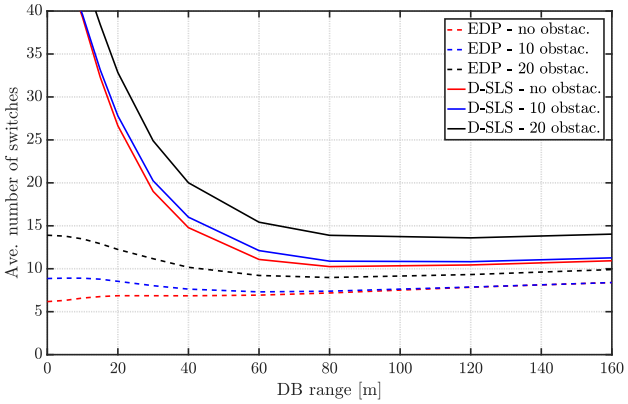

(b) $80m$ location error.

Fig. 11. Performance evaluation of DB-aided algorithms in terms of average number of beam switches varying location error and number of obstacles in the area.

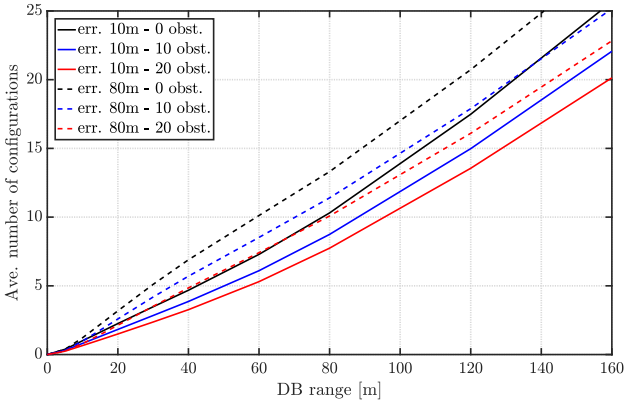

Fig. 12. Average number of DB candidate configurations varying location error and number of obstacles in the area.

be reached by a larger variety of beam configurations with respect to the case there was no location error, i.e., they were close to the nominal ones.

Fig. 13 shows the conditioned probability of successfully establishing a connection using the DB information, provided that at least one candidate DB entry is available and considered for the incoming user. The impact of the range m on the success probability is the result of a trade-off between two aspects. Increasing m causes users "relatively far" from DB entries to have non-empty candidate sets. This generally decreases the conditioned success probability because it brings in users "relatively badly positioned" with

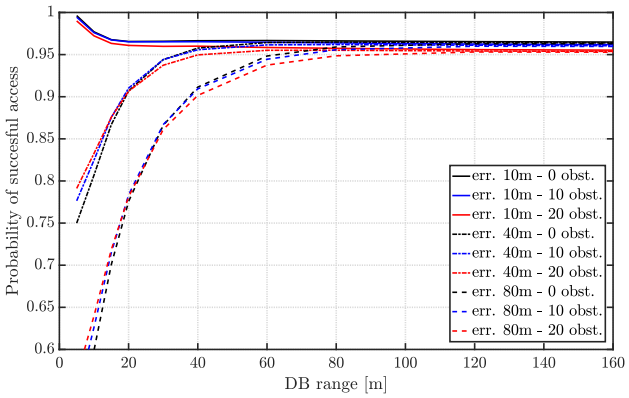

Fig. 13. Probability of successful memory access varying location error and number of obstacles in the area.

respect to DB entries. However, increasing m enlarges the set of beam configurations that can be tested when the DB is accessed, this increases the success probability, especially in case of location errors. The final emerging behavior depends on the actual numbers of obstacles and on the location error intensity, determining the curves' trend in the figure.

7 Implementation Aspects

Current cellular deployments are characterized by the lack of multi-connectivity solutions able to orchestrate and fully exploit different Radio Access Technologies to provide context-based throughput improvements. In order to address this issue, an approach based on BS-assisted networks, also known as "Phantom Cell" approach [39], has been recently proposed as a solution offering a continuous service by means of the BS (or eNodeB, according to the 3GPP terminology) coverage, while capitalizing the ultra capacity access such that provided by mm-wave small cells, as previously presented in Section 1.

The Phantom Cell concept relies on the C-plane/U-plane splitting. While the C-plane is provided by eNodeBs (eNBs) for all users within the network, the U-plane is provided by mm-wave small cells only for those users within the ultra-capacity coverage. Hence, the radio resource control (RRC) connection phase between MTs (or UEs, according to the 3GPP terminology) and the mm-wave small cells, e.g., channel establishment and release operations, are directly controlled by the eNB. Although mm-wave small cells do not provide a cell identification signals, they might be directly accessed through the eNB signaling. This benefits the control signaling in terms of handover procedures, which are significantly reduced. However, it requires low-latency connections, such as optical fibers, between the eNB and the mm-wave small cells. This architecture enables the use of mm-wave technologies in the radio access networks.

When a user crosses an ultra capacity area, it might be granted to access to the mm-wave small-cell network, as depicted in Fig. 14. The user sends the ultra capacity connection request (1.) through the control plane. The eNodeB activates the new connection procedure by issuing the ultra capacity requests towards best candidate mm-wave small cells that can cover the user (2.). After checking the resource availability, the mm-wave cell accepts the new user connection (3.). The discovery procedure starts

afterwards (5.) and, once the user is discovered, the ultra capacity connection between the mm-wave small cell and the user can be correctly established (11.). The figure also shows how this system can be fully supported by a new ICT standardization framework aiming at providing more "intelligence" towards the network edge, namely the *Mobile Edge Computing* platform [40].

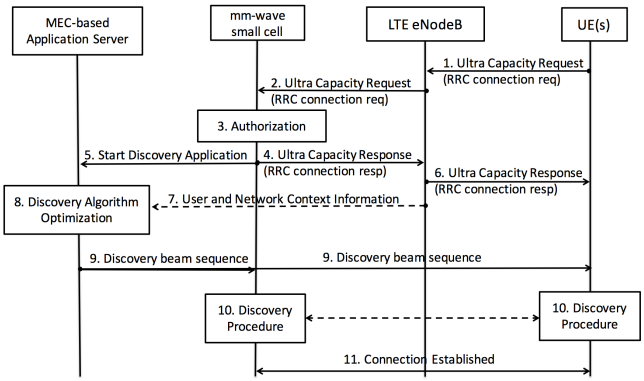

Fig. 14. Flow diagram for Cell Discovery Procedure in 3GPP architecture.

Mobile Edge Computing (MEC) is a ISG (Industry Specification Group) defined by the ETSI standardization organization, which started in 2014 from a consortium of the major industrial partners and mobile operators. The main objective of MEC is to provide an IT service environment at the edge of the network, wherein user-specific applications may be developed. The main advantage relies on the very low latency and high bandwidth which facilitate a real-time access to radio resources. The MEC platform might be placed at base stations as well as in data-centers close to the access network, to provide processing and data storage functionalities. The standardization group has the goal of defining advanced APIs, based on both network and user context, to develop network applications for increasing the user quality of experience, such as augmented reality or gaming.

In our perspective, MEC platform enables the improvement of network management operations as well, by allowing the design of advanced functionalities, computational-intensive and/or storage-demanding, operating on a local basis. Supporting mm-wave small cells with a MEC platform allows network operators to develop application-specific discovery algorithms, e.g., SLS, D-SLS or EDP, to make user and BS beam each other and provide ultra-capacity connectivity. Applications can also coordinate the activity of a pool of small cells and process large DBs of context information, gathered at different places in different times, in order to speed up the discovery.

As shown in Fig. 14, when an ultra-capacity connection request is received, the mm-wave small cell requests the activation of an instance of the Discovery Application on the MEC-based Application Server (5.), the application runs in a virtualized environment and collects user and network information via the MEC API in order to optimize the cell discovery process (7.). After the customization of the discovery phase parameters according to the specific context information (8.), the Discovery Application dispatches the best sequences of beam configuration identifiers to both small cells and users, through the C-plane connection (9.). Scanning through the provided sequences, the mm-wave small cell and the user eventually beam each other. Then, the Mobile Management Entity (MME) can starts the soft-handover: the Serving Gateway (S-GW) will instantiate a new GTP tunnel with the user through the mm-wave small cell. The ultra-capacity connection is successfully established (11.).

8 Concluding Remarks

We have analyzed the directional cell discovery problem in mm-wave 5G networks characterized by the C-/U-plane split. We have shown that currently available solutions are not suitable for mm-wave highly-directional systems and novel approaches must be designed.

We have proposed new discovery algorithms enhanced by the context-information available through the separated C-plane link. Results show that the performance of the algorithms depends on user distribution, however, they greatly outperform conventional SLS procedures, even in case of low information accuracy. In addition, we have developed an analytic model that predicts the cell discovery time with very high accuracy at both BS and MT side.

We have also investigated the beneficial impact of a geo-located context database, which can substantially improve the performance of the proposed algorithm in case of obstacles, basically enabling mm-wave cell discovery in future network scenarios.

Acknowledgments

The research leading to these results has been partially supported by the EU 7th Framework Program (FP7-ICT-2013-EU-Japan) under grant agreement number 608637 (MiWEBA).

References

[1] S. Rangan, T. Rappaport, and E. Erkip, "Millimeter-wave cellular wireless networks: Potentials and challenges," *Proceedings of the IEEE*, vol. 102, no. 3, pp. 366–385, Mar 2014.

[2] A. Maltsev, A. Pudeyev, I. Karls, I. Bolotin, G. Morozov, R. Weiler, M. Peter, and W. Keusgen, "Quasi-deterministic approach to mmwave channel modeling in a non-stationary environment," in *IEEE Globecom 2014, Workshop on Emerging Technologies for 5G Wireless Cellular Networks*, 2014.

[3] A. Ghosh, T. Thomas, M. Cudak, R. Ratasuk, P. Moorut, F. Vook, T. Rappaport, G. Maccartney, S. Sun, and S. Nie, "Millimeter-wave enhanced local area systems: A high-data-rate approach for future wireless networks," *Selected Areas in Communications, IEEE Journal on*, vol. 32, no. 6, pp. 1152–1163, Jun 2014.

[4] T. Bai and R. Heath, "Coverage and rate analysis for millimeter-wave cellular networks," *Wireless Communications, IEEE Transactions on*, vol. 14, no. 2, pp. 1100–1114, Feb 2015.

[5] A. Capone, A. F. dos Santos, I. Filippini, and B. Gloss, "Looking beyond green cellular networks," in *Wireless On-demand Network Systems and Services (WONS), 2012 9th Annual Conference on*. IEEE, 2012, pp. 127–130.

[6] Y. Niu, Y. Li, M. Chen, D. Jin, and S. Chen, "A cross-layer design for a software-defined millimeter-wave mobile broadband system," *IEEE Communications Magazine*, vol. 54, no. 2, pp. 124–130, Feb 2016.

[7] R. Weiler, W. Keusgen, I. Filippini, and A. Capone, "Split control plane functionality in millimeter-wave overlay access," in *1st International Conference on 5G for Ubiquitous Connectivity*, 2014.

[8] Q. C. Li, H. Niu, G. Wu, and R. Q. Hu, "Anchor-booster based heterogeneous networks with mmwave capable booster cells," in *Globecom Workshops (GC Wkshps)*. IEEE, 2013, pp. 93–98.

[9] V. Raghavan, J. Cezanne, S. Subramanian, A. Sampath, and O. Koymen, "Beamforming tradeoffs for initial UE discovery in millimeter-wave MIMO systems," *IEEE Journal of Selected Topics in Signal Processing*, vol. 10, no. 3, pp. 543–559, 2016.

[10] J. Palacios, D. D. Donno, and J. Widmer, "Tracking mmwave channel dynamics: Fast beam training strategies under mobility," in *IEEE INFOCOM 2017 - IEEE Conference on Computer Communications*, May 2017.

[11] A. Alkhateeb, Y. H. Nam, M. S. Rahman, J. Zhang, and R. W. Heath, "Initial beam association in millimeter wave cellular systems: Analysis and design insights," *IEEE Transactions on Wireless Communications*, vol. 16, no. 5, pp. 2807–2821, May 2017.

[12] P. Parada and M. Zorzi, "Cell discovery based on historical users location in mmwave 5G," in *European Wireless (EW) 2017*, Apr 2017.

[13] H. Shokri-Ghadikolaei, F. Boccardi, C. Fischione, G. Fodor, and M. Zorzi, "Spectrum sharing in mmwave cellular networks via cell association, coordination, and beamforming," *IEEE Journal on Selected Areas in Communications*, vol. 34, no. 11, pp. 2902–2917, Nov 2016.

[14] M. Akdeniz, Y. Liu, M. Samimi, S. Sun, S. Rangan, T. Rappaport, and E. Erkip, "Millimeter wave channel modeling and cellular capacity evaluation," *Selected Areas in Communications, IEEE Journal on*, vol. 32, no. 6, pp. 1164–1179, Jun 2014.

[15] R. Weiler, W. Keusgen, A. Maltsev, T. Kuhne, A. Pudeyev, L. Xian, J. Kim, and M. Peter, "Millimeter-wave outdoor access shadowing mitigation using beamforming arrays," in *Antennas and Propagation (EuCAP), 2016 European Conference on*, Apr 2016, pp. 4568–4573.

[16] O. Holland, "Some are born with white space, some achieve white space, and some have white space thrust upon them," *IEEE Transactions on Cognitive Communications and Networking*, vol. 2, no. 2, pp. 178–193, Jun 2016.

[17] G. Jakllari, W. Luo, and S. V. Krishnamurthy, "An integrated neighbor discovery and MAC protocol for ad hoc networks using directional antennas," *Wireless Communications, IEEE Transactions on*, vol. 6, no. 3, pp. 1114–1024, 2007.

[18] R. Choudhury, X. Yang, R. Ramanathan, and N. Vaidya, "On designing mac protocols for wireless networks using directional antennas," *Mobile Computing, IEEE Transactions on*, vol. 5, no. 5, pp. 477–491, May 2006.

[19] R. Ramanathan, J. Redi, C. Santivanez, D. Wiggins, and S. Polit, "Ad hoc networking with directional antennas: a complete system solution," *Selected Areas in Communications, IEEE Journal on*, vol. 23, no. 3, pp. 496–506, Mar 2005.

[20] T. Korakis, G. Jakllari, and L. Tassiulas, "CDR-MAC: A protocol for full exploitation of directional antennas in ad hoc wireless networks," *Mobile Computing, IEEE Transactions on*, vol. 7, no. 2, pp. 145–155, Feb 2008.

[21] R. Choudhury and N. Vaidya, "Deafness: a MAC problem in ad hoc networks when using directional antennas," in *Network Protocols, 2004. ICNP 2004. Proceedings of the 12th IEEE International Conference on*, Oct 2004, pp. 283–292.

[22] J. Wang, Z. Lan, C.-W. Pyo, T. Baykas, C.-S. Sum, M. A. Rahman, J. Gao, R. Funada, F. Kojima, H. Harada *et al.*, "Beam codebook based beamforming protocol for multi-Gbps millimeter-wave WPAN systems," *Selected Areas in Communications, IEEE Journal on*, vol. 27, no. 8, pp. 1390–1399, 2009.

[23] S. Singh, F. Ziliotto, U. Madhow, E. Belding, and M. Rodwell, "Blockage and directivity in 60 GHz wireless personal area networks: from cross-layer model to multihop MAC design," *Selected Areas in Communications, IEEE Journal on*, vol. 27, no. 8, pp. 1400–1413, 2009.

[24] K. Chandra, R. Prasad, I. Niemegeers, and A. Biswas, "Adaptive beamwidth selection for contention based access periods in millimeter wave WLANs," in *Consumer Communications and Networking Conference (CCNC), 2014 IEEE 11th*, Jan 2014, pp. 458–464.

[25] Q. Chen, J. Tang, D. Wong, X. Peng, and Y. Zhang, "Directional cooperative MAC protocol design and performance analysis for IEEE 802.11ad WLANs," *Vehicular Technology, IEEE Transactions on*, vol. 62, no. 6, pp. 2667–2677, Jul 2013.

[26] H. Shokri-Ghadikolaei, L. Gkatzikis, and C. Fischione, "Beam-searching and transmission scheduling in millimeter wave communications," in *Communications (ICC), 2015 IEEE International Conference on*, Jun 2015, pp. 1292–1297.

[27] A. Patra, L. Simić, and P. Mähönen, "Smart mm-wave beam steering algorithm for fast link re-establishment under node mobility in 60 GHz indoor WLANs," in *Proceedings of the 13th ACM International Symposium on Mobility Management and Wireless Access (MobiWac)*, 2015, pp. 53–62.

[28] A. Capone, I. Filippini, and V. Sciancalepore, "Context information for fast cell discovery in mm-wave 5G networks," in *European Wireless 2015, 21th European Wireless Conference*, May 2015.

[29] A. Capone, I. Filippini, V. Sciancalepore, and D. Tremolada, "Obstacle avoidance cell discovery using mm-wave directive antennas in 5G networks," in *IEEE PIMRC 2015, Workshop on Cloud Cooperated Heterogeneous Cellular Networks for 5G*, Aug 2015.

[30] C. Barati, S. Hosseini, S. Rangan, P. Liu, T. Korakis, S. Panwar, and T. Rappaport, "Directional cell discovery in millimeter wave cellular networks," *Wireless Communications, IEEE Transactions on*, vol. 14, no. 12, pp. 6664–6678, Dec 2015.

[31] C. Liu, M. Li, I. B. Collings, S. V. Hanly, and P. Whiting, "Design and analysis of transmit beamforming for millimeter wave base station discovery," *IEEE Transactions on Wireless Communications*, vol. 16, no. 2, pp. 797–811, Feb 2017.

[32] H. Shokri-Ghadikolaei, C. Fischione, G. Fodor, P. Popovski, and M. Zorzi, "Millimeter wave cellular networks: A MAC layer perspective," *Communications, IEEE Transactions on*, vol. 63, no. 10, pp. 3437–3458, Oct 2015.

[33] C. Barati, S. Hosseini, S. Rangan, P. Liu, T. Korakis, and S. Panwar, "Directional cell search for millimeter wave cellular systems," in *Signal Processing Advances in Wireless Communications (SPAWC), 2014 IEEE 15th International Workshop on*, Jun 2014, pp. 120–124.

[34] M. Giordani, M. Mezzavilla, C. Barati, S. Rangan, and M. Zorzi, "Comparative analysis of initial access techniques in 5G mm-wave cellular networks," in *50th Annual Conference on Information Sciences and Systems (CISS), Mar 2016*.

[35] W. B. Abbas and M. Zorzi, "Context information based initial cell search for millimeter wave 5G cellular networks," in *2016 European Conference on Networks and Communications (EuCNC)*, Jun 2016, pp. 111–116.

[36] A. Redondi, I. Filippini, and A. Capone, "Context management in energy-efficient radio access networks," in *Digital Communications-Green ICT (TIWDC), 2013 24th Tyrrhenian International Workshop on*. IEEE, 2013, pp. 1–5.

[37] "FP7-ICT-608637 MiWEBA Project Deliverable D5.1 - Channel Modeling and Characterization," Jun 2014. [Online]. Available: http://www.miweba.eu/wp-content/uploads/2014/07/MiWEBA_D5.1_v1.01.pdf

[38] A. P. Andrews, L. R. Weill, and M. S. Grewal, *Global Positional Systems, Inertial Navigation, and Integration*. John Wiley & Sons, Inc. 2001.

[39] H. ISHII, Y. Kishiyama, and H. Takahashi, "A novel architecture for LTE-B: C-plane/U-plane split and phantom cell concept," in *Globecom Workshops (GC Wkshps)*, Dec 2012, pp. 624–630.

[40] "Mobile-Edge Computing," Sept 2014. [Online]. Available: https://portal.etsi.org/Portals/0/TBpages/MEC/Docs/Mobile-edge_Computing_-_Introductory_Technical_White_Paper_V1%2018-09-14.pdf